JMEPEG (2009) 18:95–101
DOI: 10.1007/s11665-008-9267-8
©ASM International
1059-9495/$19.00

Analysis of Capacitance Characteristics of C_{60}, C_{70}, and La@C_{82}

Nick E. Tran, Samuel G. Lambrakos, and Joseph J. Lagowski

(Submitted April 3, 2008; in revised form June 3, 2008)

Fullerenes and their derivatives are promising materials for supercapacitor devices due to their unique nanostructure that combines the reversible redox charge storage with the high surface area. In this article, the reversible redox charge storage of C_{60}, C_{70}, and La@C_{82} in liquid ammonia solution is reported. An electrochemical analysis of these species using cyclic voltammetry is presented in conjunction with the theoretical interpretation. The relative magnitudes of transfer coefficients, which represent a measure of the symmetry of the energy barrier for oxidation and reduction of the monoanionic species of these fullerenes, suggest that the availability of the surface area permitting delocalization of π electrons is a determining factor of their first reduction potential. The relationship between these transfer coefficients and fullerene geometry also support previous conclusions that the La atom is located within the fullerene cage of La@C_{82}. The electrochemical measurements analyzed were made using a modified three-compartment cell. Advantages associated with this modified cell for analysis of capacitance characteristics of C_{60}, C_{70}, and La@C_{82} are discussed.

Keywords advanced characterization, chemical analysis, energy

1. Introduction

Hybrid electric vehicles require batteries that can supply bursts of power to a gasoline engine. The problems with these batteries are that they possess low power density and lose an average of 20% input energy from chemical reactions. Supercapacitors are more powerful and more efficient than batteries because their energy is stored in an electric field. The energy storage capacity of supercapacitors, however, is relatively low. The energy density of commercial supercapacitors is around 6 Wh/kg, compared to 120 Wh/kg for lithium-ion batteries of similar sizes. The energy density of a supercapacitor is proportional to the surface area of its electrodes, which are often fabricated from activated carbon due to its large specific surface area (≈700 m^2/g). In addition to being more chemically stable and more uniform in sizes and shapes, fullerenes and their derivatives also have larger specific surface areas (see Table 2 below) than the activated carbon. Because of these factors, fullerenes and their derivatives are believed to be superior materials to activated carbon for the fabrication of supercapacitor's electrodes. This report examines how the size and shape of fullerenes, and related species, influence their reversible redox charge storage and other electrochemical properties.

Nick E. Tran, Department of Chemistry, George Washington University, Washington, DC 20052; **Samuel G. Lambrakos**, Materials Science and Component Technology Directorate, Naval Research Laboratory, Washington, DC 20375; and **Joseph J. Lagowski**, Department of Chemistry and Biochemistry, University of Texas at Austin, Austin, Texas 78712. Contact e-mail: nicketran@gmail.com.

The electrochemistry of empty fullerenes (Ref 1-8) and endohedral metallofullerenes (Ref 9-11) shows that their electrochemical properties are strongly affected by solute-solvent interactions. The dependence of the electrochemical properties of fullerenes on their size and geometry, however, has not been investigated. In this study, the cyclic voltammetry of empty fullerenes (C_{60}, C_{70}) and an endohedral metallofullerene (La@C_{82}) in liquid ammonia solution is reported and the symmetry of the energy barrier for oxidation and reduction of the monoanionic species of these fullerenes is analyzed using Tafel plots. The relative magnitudes of transfer coefficients (the quantity α defined below) obtained from this analysis are correlated with the relative cage geometries and other physical properties of the fullerenes. This correlation supports implications concerning the effect of delocalized electrons on the redox potentials of the fullerenes, and the location of La relative to the C_{82} cage, which has been previously investigated (Ref 12, 13).

Although employing basically the same electrochemical techniques, the electrochemistry of C_{60} in liquid ammonia solution presented in this study is different than the previously published data (Ref 5). Unlike the previous study, KCF_3SO_3 was used in this study as the electrolyte instead of KI because it is more electrochemically stable in liquid ammonia solution.

The electrochemical measurements are made using a modified three-compartment cell. A significant feature of this cell is its ability to minimize the effect of the potential drift, which often occurs during the course of long experiments involving extensive reduction of the fullerene species.

2. Experimental

2.1 Instrumentation

The electrochemical experiments analyzed in this study were performed using a modified three-compartment cell (Fig. 1).

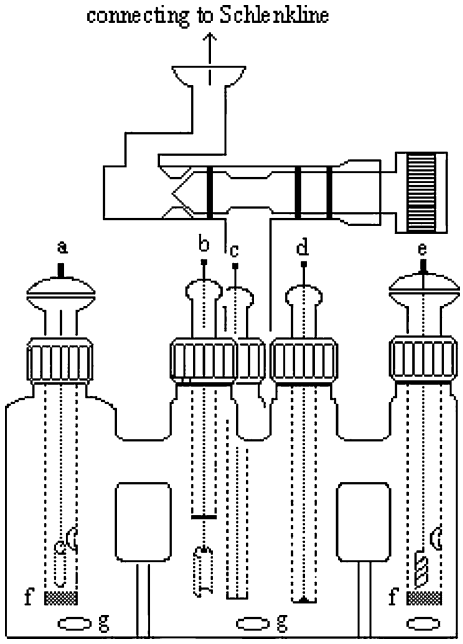

Fig. 1 A modified three-compartment electrochemical cell. (a) Platinum cylinder auxiliary electrode; (b) platinum plate working electrode; (c) platinum ultramicro working electrode; (d) platinum microdisk working electrode; (e) pseudo-reference electrode; (f) fritted glass; (g) stir bar

This cell consists of an ultramicro platinum working electrode, a platinum plate working electrode, a platinum microdisk working electrode, a platinum cylinder auxiliary electrode, and a pseudo-reference electrode.

The ultramicro working electrode was fabricated by cementing a platinum filament (2 cm length, 25 μm diameter, 99.95%, Johnson Matthey) to a chromel wire (18 cm) with silver epoxy (Epoxy Technology Inc.). The platinum filament was sealed inside a soft glass tube (7 mm outside diameter, 1 mm inside diameter, 22 mm long) by passing a gentle O_2 flame over the glass. The tip of the platinum electrode was then polished with four grades of Metadi II diamond polishing powder of particle size 6, 3, 1, and 0.25 μm, sequentially, until the surface of the electrode tip acquired a mirror-like appearance. The microdisk electrode was prepared by melting the end of a platinum wire (20 cm length, 0.50 mm diameter, 99.95%, Johnson Matthey) into a sphere. The platinum wire was then sealed inside a glass tube and then ground mechanically until only the half of the sphere, which was embedded in the glass, remained.

The tip of the platinum was polished with diamond polishing powder using the same technique described for the ultramicro working electrode. The projected surface area of the microelectrode [0.0031 ($\pm$0.0001 cm^2)] was determined by chronocoulometry, which uses an aqueous solution of (3.2 mM) $Fe(CN)_6^{3-}$ and (1 M) KCl. Before each experiment, the microdisk and the ultramicro electrodes were electrocycled in (1 M) H_2SO_4 until their oxidation and reduction waves were stable. Using potentials between +1.15 and −0.65 V (vs. a saturated mercurous sulfate electrode, SMSE), this process usually took approximately 10 min.

The pseudo-reference electrode was a silver wire (3 cm long, 0.5 mm diameter, 99.9985%, Johnson Matthey), the lower section of which was wound into a cylindrical helix to increase the contacted surface area between the electrode and its solution. At the beginning of each experiment, the pseudo-reference electrode was dipped into a diluted solution of nitric acid until a white powder of $AgNO_3$ coated its surface. The reference electrode was then dried in an oven. The auxiliary electrode contained a (1.0 × 0.5 cm) platinum cylinder, which was spot-welded to a platinum wire.

The design of the modified electrochemical cell allowed the height of the electrodes to be adjusted according to the level of the solution inside the cell. The level of the solution inside the glass compartment that housed the reference electrode (Fig. 1) was always kept higher than that of the cell. This minor innovation helped to keep the solution contained within the reference compartment unchanged, thus minimizing the potential drift, which often occurred during the course of a long experiment.

Some experiments in this study required the coulometric generation of solvated electrons in liquid ammonia solutions. These experiments were carried out with an EG&G PARC Model 175 Universal programmer used in tandem with an EG&G Princeton Applied Research Model 173 Potentiostat/Galvanostat. The remainder of the electrochemical experiments were conducted with a Model 273A Potentiostat/Galvanostat (EG&G Princeton Applied Research Corporation), where the device was driven by PARC Model 270 Electrochemical Analysis System software which was coupled with an IBM PS/2 Model 55ST.

2.2 Chemicals

All the electrochemical experiments in this study were performed in an inert environment of dried He gas. The liquid ammonia solvent (La Roche industries inc., premium grade) was dried with sodium before being used. About 1 g of sodium (Johnson Matthey, 99.9%) was cut into small pieces and washed three times with hexanes. The sodium was added to a round bottom flask, which was connected to a Schlenk line. About 120 mL of liquid ammonia was then condensed into the flask and the mixture was stirred vigorously for at least an hour. The flask of sodium-ammonia solution was then frozen (by liquid nitrogen), evacuated, and then refilled with dried He gas. This process was repeated three times to remove volatile substances, such as the hydrogen and oxygen formed during the reaction between the solvated electrons and water in the system. After the solvent was appropriately dried, a small portion (1 mL) of the solution was condensed into the electrochemical cell. This condensation could be accomplished by allowing the liquid ammonia in the drying flask to be warmed up to room temperature, while the cell was simultaneously cooled by a low temperature bath of IPA (isopropyl alcohol) and dry ice. The dried ammonia coated the walls of the electrochemical cell and the electrolyte, potassium triflate (potassiumtrifluoromethylsulfonate, KCF_3SO_3, Johnson Matthey, 98%), contained therein. The ammonia solvent was then evaporated from the cell by a heat gun. The cell was "sweated" twice in this way to remove any trace of water, which adsorbed quite strongly on the cell walls. About 100 mL of ammonia was finally condensed into the electrochemical cell to make a 0.1 M KCF_3SO_3-NH_3 solution (KCF_3SO_3 is a more stable electrolyte than KI in liquid NH_3). The solution was then scanned by cyclic voltammetry to detect impurities. If the baseline of the solution was similar to that shown in Fig. 2, then a sample of fullerene could be introduced into the solution. The base line scan of the KCF_3SO_3-NH_3 solution was observed to always consist of two

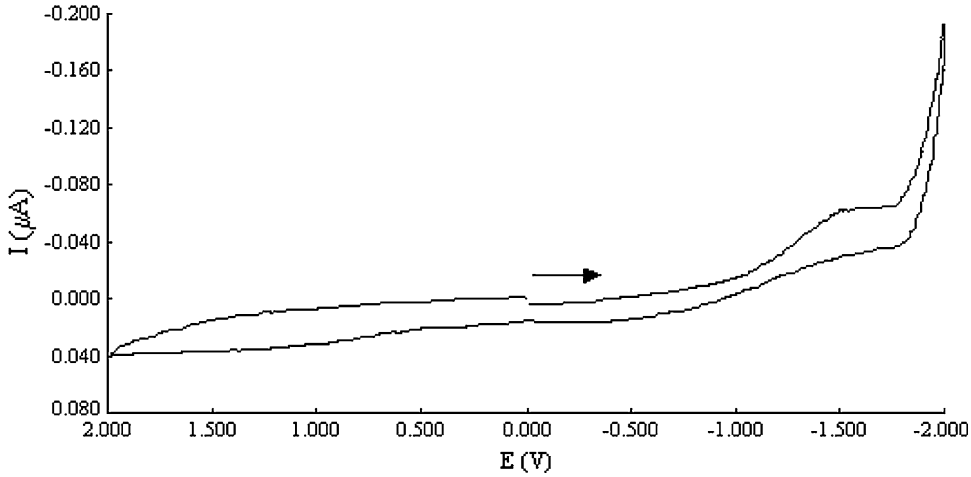

Fig. 2 Baseline scan of a (0.1 M) NH_3-KCF_3SO_3 solution at −50 °C. The working electrode was a platinum microdisk electrode (0.0031 ± 0.0001 cm^2), the pseudo-reference electrode was $Ag/Ag(NO_3)$, and the counter electrode was a platinum cylinder. The scan rate was 200 mV/s. The arrow indicates the scanning direction

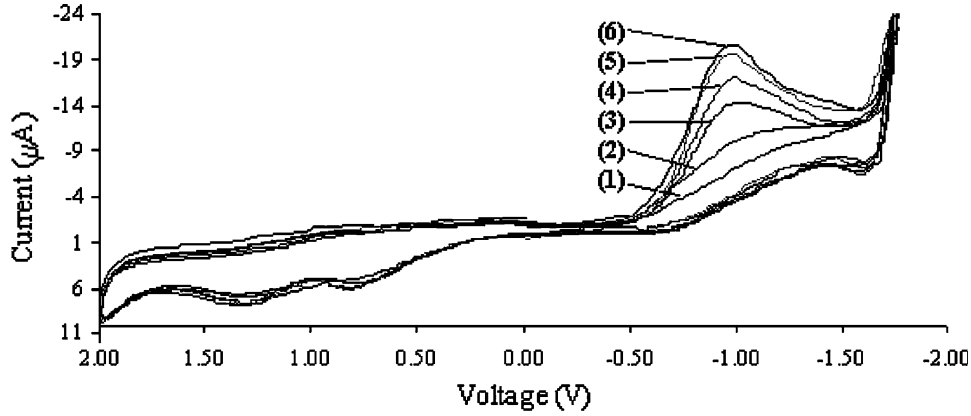

Fig. 3 Cyclic voltammogram of a 1.0 mM C_{60}^- liquid NH_3 solution with 0.1 M KCF_3SO_3 at −50 °C. The scan rate was 200 mV/s

reduction waves. The reduction wave at −1.49 V (Fig. 2) was attributed to the unknown impurity in KCF_3SO_3 electrolyte, which was only 98% pure. The reduction wave at −1.76 V was attributed to the solvent limit of NH_3. Solvated electrons are produced at this potential in (0.1 M) KCF_3SO_3/NH_3 solution.

The species C_{60}, C_{70}, and LaC_{82} were synthesized by arcing La-doped carbon rods in a modified carbon arc reactor (Ref 14). The products were separated from the rest of the carbon soot by Soxhlet extraction in an inert atmosphere of dried He. The extracted products, C_{60}, C_{70}, and LaC_{82}, were separated from each other simultaneously using an ionization coupled chromatographic technique (ICC) (Ref 15).

2.3 The Cyclic Voltammetry of C_{60}, C_{70}, and La@C_{82} in Liquid Ammonia Solution

2.3.1 C_{60}. A sample of 5.0×10^{-5} moles of C_{60} obtained from the ICC experiments was introduced into a KCF_3SO_3-NH_3 solution under an over pressure of He gas. The liquid ammonia solution in all three compartments was stirred vigorously for half an hour in order to break up the fullerene powder. The initial cathodic and anodic scans of this mixture, C_{60} in NH_3-KCF_3SO_3 solution, showed a similar cyclic voltammogram to Fig. 2, indicating that C_{60} is not soluble in the NH_3-KCF_3SO_3 solution. About 7.3×10^{-5} moles of solvated electrons (e_s) was then introduced into the mixture contained in the working compartment by passing a −2.8 V electric current through the platinum sheet electrode (Fig. 1). It was found that 7.3×10^{-5} moles of e_s was sufficient for converting the entire sample of fullerene into the corresponding monoanion fullerene species C_{60}^-. The solution containing C_{60}^- and solvated electrons was stirred for approximately an hour and then subjected to cyclic voltammetry. The cathodic and anodic sweeps were limited between +2.000 and −1.75 V. The cyclic voltammogram (CV) of the solution (Fig. 3) showed a large reduction peak at −0.96 V, which is ascribed to the reduction of C_{60} to C_{60}^{1-}. This peak was initially absent in the first cathodic sweep but appeared in the subsequent cathodic sweeps, an indication that C_{60}^- in the ammonia solution was oxidized and deposited onto the surface of the electrode as thin film during the reversed anodic sweeps. The oxidation wave of C_{60}^- to C_{60} (−0.89 V) was observed during the initial reversed anodic sweep. The peak intensity, however, became progressively weaker as each subsequent scan was taken, indicating

Table 1 The peak potentials (first row) and half-cell potentials (second row) of C_{60}, C_{70}, and La@C_{82} in (0.1 M) KCF_3SO_3-NH_3 solution at −50 °C

Samples	Scan rate, mV/s	Solvent/electrolyte	$^{ox}E_1$, V	$^{ox}E_2$, V	$^{re}E_1$, V	$^{re}E_2$, V
C_{60}	200 (Ag/$AgNO_3$)	NH_3/KCF_3SO_3	+1.30	+0.76	−0.96	−1.43
			+1.26	+0.54	−0.89	−1.38
C_{70}	200 (Ag/$AgNO_3$)	NH_3/KCF_3SO_3	+1.31	+0.74	−0.94	
			+1.28	+0.70	−0.86	
La@C_{82}	200 (Ag/$AgNO_3$)	NH_3/KCF_3SO_3	+1.43	+0.92	−0.72	
			+1.39	+0.89	−0.64	

The exact potential was not determined due to background current

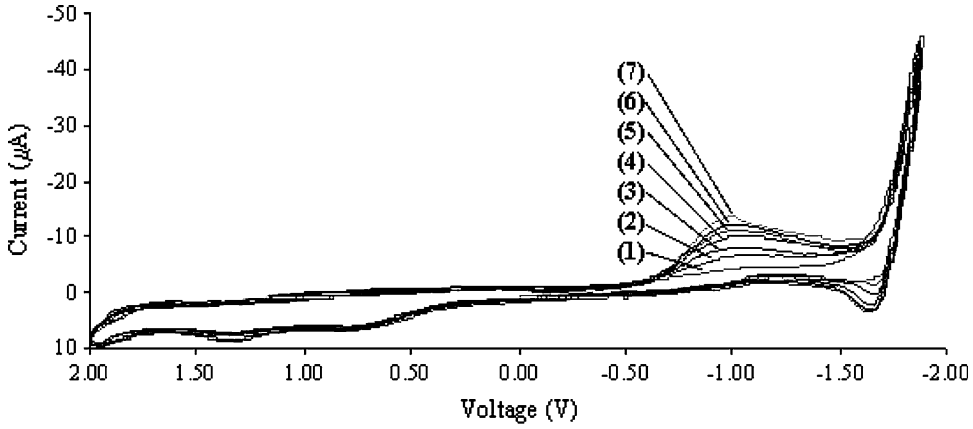

Fig. 4 Cyclic voltammogram of (1.0 mM) C_{70}^- in liquid NH_3 with 0.1 M KCF_3SO_3 at −50 °C. The scan rate was 200 mV/s

that C_{60} may act as an insulating layer on the electrode surface. Other small oxidation and reduction peaks that were observed for C_{60}^- are given in Table 1.

2.3.2 C_{70}. A (1.0 mM) C_{70}^- NH_3 solution was prepared in the same way as the C_{60}^- NH_3 solution described above. The cyclic voltammetry of the C_{70}^- NH_3 solution (Fig. 4) showed a reduction of C_{70} to C_{70}^- at −0.94 V, almost at the same location as the reduction of C_{60} to C_{60}^- (−0.96 V). Like the oxidation of C_{60}^- to C_{60}, the oxidation wave of C_{70}^- to C_{70} (−0.86 V) was observed during the initial reversed anodic sweep. The peak intensity of this wave, however, became obscure as more C_{70} was deposited on the working electrode surface. Due to the lack of a responsive and well-defined oxidation wave in the CV of $C_{70,}$ as shown above, it is difficult to determine the exact number of electrons involved in the first reduction of C_{70} without more electrochemical experiments. Accordingly, it was assumed that the first reduction of C_{70} is due to a one-electron process. This assumption is based on the fact that previous experiments involving the reduction of empty fullerenes in various solvents have never indicated otherwise (Ref 1-8). Other redox potentials C_{70} were also observed, occurring at approximately the same locations as those of the C_{60} (Table 1).

2.3.3 La@C_{82}. The electrochemistry of La@C_{82} in liquid ammonia solution was studied using the same procedures applied to the C_{60} electrochemical experiments. A 100 mL of 9.0×10^{-6} M La@C_{82}/toluene faint yellow solution was introduced into the electrochemical cell before each experiment. Approximately 1.4×10^{-5} moles of e_s was introduced into the solution, enough to convert all the La@C_{82} into La@C_{82}^- species. The solution was stirred for about an hour and then cyclic voltammetry was performed on the solvated electron solution of ammonia and La@C_{82}^-. The cathodic and anodic sweeps were limited between +2.000 V and −1.800 V at a scan rate of 200 mV (Fig. 5). The cyclic voltammogram (CV) of the solution showed distinctly one reduction and two oxidation waves. The first reduction potential of La@C_{82}^0 to La@C_{82}^- on the forward cathodic scan was observed at −0.723 V, which was 240 mV more positive than the reduction of C_{60} to C_{60}^- in liquid ammonia solution (Table 1). On separate scans (at 200 mV/s scan rate between +2.000 V and −0.500 V) weak peaks at +0.86 V and +1.35 V were detected, indicating the possible reduction of La@C_{82}^+ to La@C_{82}^0 and La@C_{82}^{2+} to La@C_{82}^+, respectively.

3. Results and Discussion

3.1 Redox Properties of C_{60}, C_{70}, La@C_{82}

In liquid ammonia solution both C_{60} and C_{70} showed electrochemical properties similar to those reported for other solvents (Ref 1, 3, 4, 6, 7). C_{60} and C_{70} show almost the same first reduction potentials, −0.96 and −0.94 V, respectively. The fact that C_{70} has fewer pyracylene bonds than C_{60} probably explains why it is less electronegative than C_{60}. Referring to Fig. 3 and 4, it also appears that C_{60} is more electrochemically reactive than C_{70}.

The CV of La@C_{82} in liquid ammonia solution revealed that its first reduction potential was 240 mV more electropositive than that of C_{60}, indicating that La@C_{82} is a stronger electron acceptor than both C_{60} and C_{70}. Since the formal charge on the

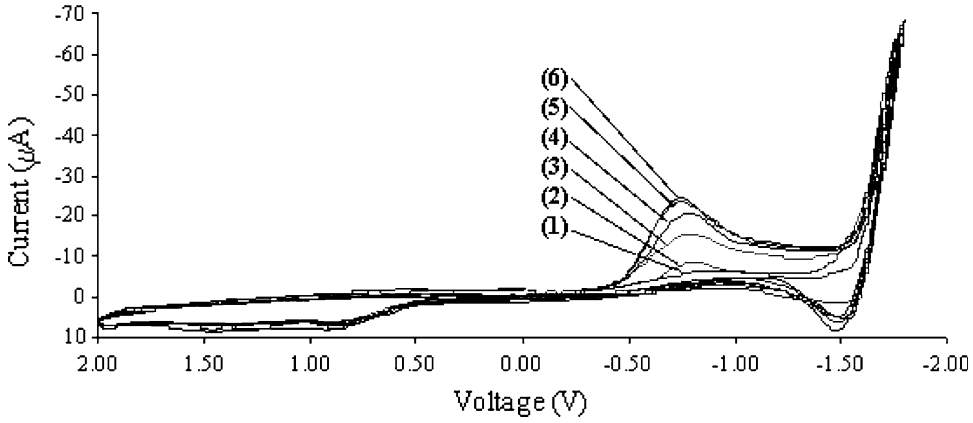

Fig. 5 Cyclic voltammogram of a 0.009 mM La@C_{82}^- liquid NH_3 solution with 0.1 M KCF_3SO_3 at −50 °C. The scan rate was 200 mV/s

Table 2 Physical and kinetic properties of Fullerenes

Fullerenes (geometry)	α	Volume, Å^3	Surface area, Å^2	Specific surface area, m^2/g[a]
C_{60} (sphere)	0.157	186.5	157.8	1364
C_{70} (prolate spheroid)	0.175	205.2	166.5	1234
C_{82} (C_{2v}, prolate spheroid)	0.218	239.8	186.8	1182

[a]Specific surface area of commercial activated carbon is approximately 700 m^2/g

La@C_{82} is already 3−, La has shown in EPR experiments to donate up to 3 of its outer electrons to the fullerenes cage (Ref 12), La@C_{82} is expected to have lower electron affinity than C_{70} and C_{60}. Our electrochemical data on La@C_{82} in liquid ammonia solution indicate that the rehybridization of C_{82} electronic structure by the electrons from the La atom makes it easier for the La@C_{82} to accept an electron than other empty fullerenes. As the result of this reduction, La@C_{82} would form a closed shell stable species, La@C_{82}^-.

The CV of La@C_{82} (Fig. 5) also revealed that the presence of C_{60} and C_{70} in the sample was much smaller than first believed; the first reduction wave of these two fullerenes was not detectable on the CV scans. The MS analysis of the La@C_{82} sample before the electrochemical experiments revealed that it contained over ten percent of these two empty fullerenes (Ref 15). The high concentration of the empty fullerenes found in the MS data is probably due to the fact that these species are much easier to evaporate than La@C_{82}.

3.2 Initial Analysis of Electrode Kinetics

The following analysis of the electrode kinetics is based on the Butler-Volmer formulation (Ref 16), according to which the electrode current i is given by the expression

$$i = nFAk_0\left[C_O e^{-\alpha nf(E-E^0)} - C_R e^{(1-\alpha)nf(E-E^0)}\right] \quad \text{(Eq 1)}$$

where the transfer coefficient (α) is a measure of the symmetry of the energy barrier between the oxidant and reductant, $f = F/RT$ (38.92 V^{-1}), and C_O and C_R are the surface concentrations of the oxidants and reductants, respectively. The quantities n, F, A, and k_0 are the number of electrons, the charge on one mole of electrons, the frequency factor which is correlated with the probability of electron transfer, and the intrinsic heterogeneous rate constant, respectively. The relationship between the value of α and the symmetry of the energy barrier is described schematically by Fig. 3.3.4 of Bard and Faulkner (Ref 16) assuming the following simple processes:

$$O + ne \xrightarrow{k_f} R \quad \text{and} \quad O + ne \xleftarrow{k_b} R \quad \text{(Eq 2)}$$

where $k_f = k_0 e^{-\alpha nf(E-E^0)}$ and $k_b = k_0 e^{(1-\alpha)nf(E-E^0)}$. In this analysis values of α are obtained by fitting Tafel plots of the cathodic branches of the current-potential curves to the first term of Eq 1 at overpotentials in the Arrhenius region, the kinetic control region, of the i vs $(E-E^0)$ curve. The large negative deviations from linearity at high $(E-E^0)$, which is correlated with the diffusion controlled part of the plot, are excluded. The values of α are given in Table 2.

It is significant to note that there was no assumption of a system whose physical characteristics are purely those of species homogeneously distributed either in solution or on film. Accordingly, the use here of Tafel plots is not to be interpreted relative to the analyses of these types of systems, but rather systems characterized in general by a metal/film/solution interface structure (Ref 17-19). The analysis considered here concerns the influence on charge transfer resulting from the presence of the large-scale cage structure defined by fullerenes at the electrode surface. A consistent assumption is that the size of fullerenes, whose characteristic scale is large relative to that of intermolecular reaction cross sections, imposes delocalization influences, effecting the rate of electron transfer. Formally, this delocalization does impose an asymmetric influence on the activation barrier, although this influence should not be associated physically with intermolecular reaction coordinates. It follows then that an interpretation of the relative magnitudes of the transfer coefficients as a measure of the symmetry of an energy barrier can be based purely on the formal mathematical structure of the Arrhenius-rate representation defined by Eq 1 given the assumption of a dominant rate determining process

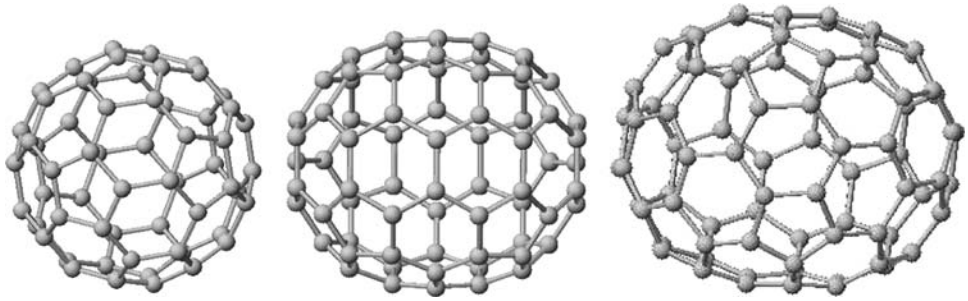

Fig. 6 Schematic presentation of C_{60}, C_{70}, and C_{82} (C2v symmetry). The diameter (in Å) of the fullerenes in *x*, *y*, and *z* Cartesian coordinates are: C_{60} = 7.09; C_{70} = 7.96, 7.02, 6.87; and C_{82} = 8.04, 8.10, 7.53, respectively

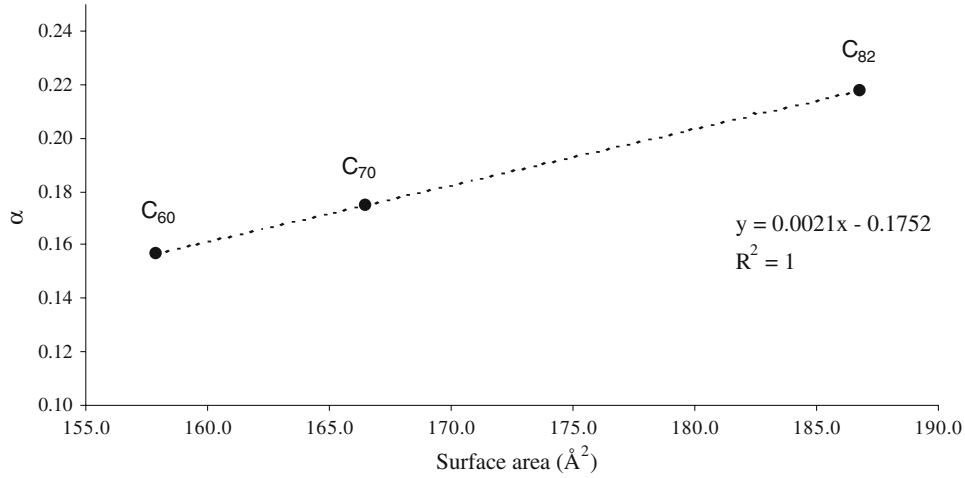

Fig. 7 Surface area of fullerene vs. transfer coefficient (α)

for a given range of overpotentials. This concept and its application has been examined by Sun and Nowak (Ref 20).

Referring to Table 2, it is noted that the values of the transfer coefficient α are all less than 0.5, implying, according to theory, that the gradient of the standard free energy with respect to the reaction coordinates is larger for the reductants than for the oxidants. It is reasonable to assume that this asymmetry of the energy barrier for oxidation and reduction can be correlated with the molecular geometry of the fullerenes and the influence of this geometry on the nature of the electron transfer in solution. Accordingly, the relationship between the transfer coefficient α and the molecular geometry of the fullerenes could be investigated by considering the fullerene carbon cages (Fig. 6), to within a reasonable level of approximation, as spherical conducting cages. Among the physical characteristics of spherical conducting cages are electron screening, which can influence electron transfer, and delocalization of electrons, which is due to the relatively large surface area of the molecules. Therefore, the relationship between α and the average surface area of the fullerene carbon cages could be established, as described in Fig. 7.

A significant implicit feature of the perfect linear trend (R^2 = 1.00) shown in Fig. 7 is that it does not indicate the participation of any reaction pathways other than those associated with the unique closed structure characteristic of carbon cages. In addition, plots of α as a function of various other physical properties of the fullerenes (Table 2) also show similar linear relationships. The functional dependence of the transfer coefficient α on the physical properties of fullerenes such as volume, number of carbon atoms, and surface areas above suggests that these fullerenes can be characterized as closed conducting structures and that the location of La in the LaC_{82} must be endohedral and not exohedral. It is plausible that an active site for electron transfer, located external to the carbon cage, such as an exohedral La atom, would not be susceptible to screening or, for that matter, any scaling commensurate with the total surface areas of C_{82} with respect to that of C_{60} and C_{70}.

The trend observed in Fig. 7 suggests that the relative level electron screening influencing electron transfer to and from the electrofullerenes is proportional to their surface area and is independent of the number of delocalized electrons on their surface. This implies that the surface area of the carbon cages are either large enough for the delocalized π electrons to not show any observable effect or that La exists within the C_{82} cage as a neutral species and not as La^{3+} as the previous EPR experiments suggested (Ref 12).

4. Conclusions

The properties of fullerenes presented in this study are relevant for the potential processing of materials used for supercapacitor devices where charge storage and transfer characteristics, i.e., capacitance characteristics, must be quantified.

This study has shown that C_{60} and C_{70} exhibit almost the same first reduction potential in (0.1 M) KCF_3SO_3-NH_3 solution (−0.96 and −0.94 V, respectively). In a similar solution the first reduction potential of La@C_{82} is −0.72 V, indicating that La@C_{82} is a stronger electron acceptor than both C_{60} and C_{70}. The lower first reduction potential of La@C_{82} also implies that the rehybridization of C_{82} electronic structure, by the three electrons donated by La atom, makes it easier for the La@C_{82} to accept an electron than other empty fullerenes. The result of this one electron reduction of La@C_{82} is a closed shell stable species, La@C_{82}^{-}.

As an extension of the CV studies, the symmetry of the energy barrier between the neutral and monoanionic species of these fullerenes has been investigated using an analysis based on Tafel plots. It appears that the transfer coefficients (α) obtained from this analysis depend linearly on the surface area of the fullerene. This trend suggests that these fullerenes are closed conducting structures and that the location of La is endohedral and not exohedral to the LaC_{82} cage. Accordingly, it is plausible to assume that La exists within the C_{82} cage as La^{3+}.

Acknowledgments

We gratefully acknowledge the support of the Naval Research Laboratory, and the postdoctoral fellowship program of the American Society for Engineering Education.

References

1. L. Echegoyen and L.E. Echegoyen, Electrochemistry of Fullerenes and Their Derivatives, *Acc. Chem. Res.*, 1998, **31**, p 593–601
2. D. Dubois, G. Moninot, W. Kutner, M.T. Jones, and K.M. Kadish, Electroreduction of Buckminsterfullerene, C_{60}, in Aprotic Solvents: Solvent, Supporting Electrolyte and Temperature Effects, *J. Phys. Chem.*, 1992, **96**, p 7137–7145
3. D. Dubois, K.M. Kadish, S. Flanagan, R.E. Haufler, L.P.F. Chibante, and L.J. Wilson, Spectroelectrochemical Study of the C_{60} and C_{70} Fullerenes and Their Mono-, Di-, Tri- and Tetraanions, *J. Am. Chem. Soc.*, 1991, **113**, p 4364–4366
4. P.-M. Allemand, A. Koch, and F. Wudl, Two Different Fullerenes Have the Same Cyclic Voltammetry, *J. Am. Chem. Soc.*, 1991, **113**, p 1050–1051
5. F. Zhou, C. Jehoulet, and A.J. Bard, Reduction and Electrochemistry of C_{60} in Liquid Ammonia, *J. Am. Chem. Soc.*, 1992, **114**, p 11004–11006
6. Q. Xie, F. Arias, and L. Echegoyen, Electrochemically-Reversible, Single-Electron Oxidation of C_{60} and C_{70}, *J. Am. Chem. Soc.*, 1993, **115**, p 9818–9819
7. Q. Xie, E. Perez-Cordero, and L. Echegoyen, Electrochemical Detection of C_{60}^{6-} and C_{70}^{6-}: Enhanced Stability of Fullerides in Solution, *J. Am. Chem. Soc.*, 1992, **114**, p 3978–3980
8. Q. Li, F. Wudl, C. Thilgen, R.L. Whetten, and F. Diederich, Unusual Electrochemical Properties of the Higher Fullerene, Chiral C_{76}, *J. Am. Chem. Soc.*, 1992, **114**, p 3994–3996
9. T. Suzuki, K. Kikuchi, F. Oguri, Y. Nakao, S. Suzuki, Y. Achiba, K. Yamamoto, H. Funasaka, and T. Takahashi, Electrochemical Properties of Fullernolanthanides, *Terahedron*, 1996, **52**(14), p 4973–4982
10. T. Suzuki, Y. Maruyama, and T. Kato, Electrochemical Properties of La@C_{82}, *J. Am. Chem. Soc.*, 1993, **115**, p 11006–11007
11. N. Nakashima, M. Sakai, H. Murakami, T. Sagara, T. Wakahara, and T. Akasaka, Construction of a Metallofullerene La@C_{82}/Artificial Lipid Film-Modified Electrode Device and Its Electron Transfer, *J. Phys. Chem. B*, 2002, **106**, p 3523–3525
12. R.D. Johnson, M.S. de Vries, J. Salem, D.S. Bethune, and C.S. Yannoni, Electron Paramagnetic Resonance Studies of Lanthanum-Containing C_{82}, *Nature*, 1992, **355**, p 239–240
13. S. Suzuki, S. Kawata, H. Shiromaru, K. Yamauchi, K. Kikuchi, T. Kato, and Y. Achiba, Isomers and Carbon-13 Hyperfine Structures of Metal-encapsulated Fullerenes M@C_{82} (M = Sc, Y, and La), *J. Phys. Chem.*, 1992, **96**, p 7159–7161
14. N.E. Tran and J.J. Lagowski, A Study of the Synthesis of Endohedral Metallofullerenes and Empty Fullerenes by the Carbon-Arc and RFICP Technique, *Carbon*, 2002, **40**, p 939–948
15. N.E. Tran, "The Synthesis, Characterization, and Electrochemistry of Endohedral Metallofullerenes", Ph.D. Dissertation, The University of Texas, Austin, TX, 2000
16. A.J. Bard and R. Faulkner, *Electrochemical Methods: Fundamentals and Applications*. John Wiley and Sons, New York, 1980
17. K.J. Vetter and F. Gorn, Kinetics of Layer Formation and Corrosion Processes of Passive Iron in Acid Solutions, *Electrochim. Acta*, 1973, **18**, p 321–326
18. N. Cabrera and N.F. Mott, Theory of the Oxidation of Metals, *Rep. Prog. Phys.*, 1948/49, **12**, p 163–184
19. R. Kirchheim, Growth Kinetics of Passive Films, *Electrochim. Acta*, 1987, **32**(11), p 1619–1629
20. E.X. Sun and W.B. Nowak, Electrochemical Characteristics of Ti-6Al-4V Alloy in 0.2 N NaCl Solution I. Tafel Slopes in Quasi-passive State, *Corros. Sci.*, 2001, **43**(10), p 1801–1816